

AD-A247 917

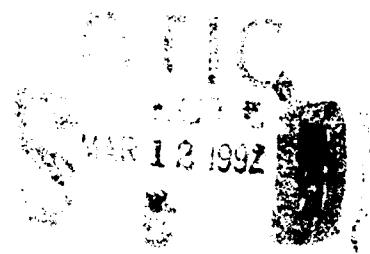


2

A Coupled Regional Tide Model

J. K. Lewis
G. A. Vayda
Science Applications International Corp.
Bay St. Louis, MS 39520

Y. L. Hsu
Mapping, Charting, and Geodesy Division
Ocean Science Directorate



Approved for public release; distribution is unlimited. Naval Oceanographic and Atmospheric Research Laboratory, Stennis Space Center, Mississippi 39529-5004.

92-06227



185

ABSTRACT

Two-dimensional numerical models were used to further study appropriate conditions at the open boundaries for regional models forced by parameters from a global tidal model. The open boundary condition of Reid and Bodine (1968) was applied to regional models of the western Florida shelf, north-central Gulf of Mexico, and the Kenya Coast. In addition, two semienclosed basins were modeled, the Persian Gulf, and the entire Gulf of Mexico.

A number of tests were conducted to determine how well forcing, using the tidal constants from the $1^\circ \times 1^\circ$ Schwiderski global model (1981, 1983) could reproduce regional tides as determined from observations. As seen in our previous work, the Reid and Bodine formulation was quite effective in driving the regional models while still allowing wave energy to propagate through the open boundaries and out of the model.

The western Florida shelf is known to resonate with the M_2 tide. Under such circumstances, the bottom friction becomes quite important in obtaining correct predictions of the observed tidal amplitudes. Several bottom friction schemes with varying drag coefficients were tested for both the north-central gulf and Florida shelf models. The results are discussed in light of the fact that we seek one scheme that would be applicable for both resonant and nonresonant situations.

In the basin modeling experiments, the M_2 tide could not be reproduced by forcing with just the Schwiderski tidal constants at the open boundaries. Perhaps the most significant problem with the Persian Gulf is the fact that it is not included in Schwiderski's global model. As for the entire Gulf of Mexico, direct gravitational forcing of the water is found to be critically important. Apparently the effect of this direct gravitational forcing does not result in a large enough signal at the Yucatan and Florida Straits such that this basin-wide model can be reproduced by forcing only at these two open boundaries.

ACKNOWLEDGMENTS

This work was supported through the Office of Naval Technology, under program element 0602435N, Dr. Thomas Warfield, program manager.

The comments from Drs. Robert Reid and Ernst Schwiderski are gratefully acknowledged.

Accession For	
NEED CLASS	<input checked="" type="checkbox"/>
INDEXED	<input type="checkbox"/>
FILED	<input type="checkbox"/>
JUL 1983	
Dr. [Name]	
[Address]	
[City, State, Zip]	
[Phone Number]	
[Fax Number]	
[E-mail Address]	
[Signature]	
[Date]	
A-1	

A Coupled Regional Tide Model

INTRODUCTION

In a previous study on the modeling of ocean tides, Lewis and Hsu (1990) pursued the topic of developing a methodology by which the tidal phases and amplitudes of a coarse grid global model could be used for forcing along the open boundaries of a relatively small, fine grid, regional model. The regional model would then be able to provide greater detail on the spatial variations of tidal amplitudes and phases. Such information is often of great value in the planning of bathymetric surveys, the determination of appropriate sampling strategies, and the spacing of tide gauges and current meter arrays.

Lewis and Hsu (hereafter, L&H) used the Reid and Bodine (1968) open boundary condition to both force a regional model of the north-central Gulf of Mexico (GOM) and allow any reflected energy to radiate out through the open boundaries. The forcing parameters came from the $1^\circ \times 1^\circ$ global model of Schwiderski (1981, 1983). The regional model was a linearized, vertically integrated, hydrodynamic model with bottom friction inversely proportional to the depth squared. L&H found that the Reid and Bodine (hereafter, R&B) boundary condition was quite effective in driving the model and in reproducing observed tidal amplitudes and phases along the Texas, Louisiana, and Mississippi Coasts. Also, factors related to the application of the R&B boundary condition were noted by L&H. First, the R&B boundary condition is based on linear wave theory and should be used with models that have grid spacings of ≤ 28 km. This restriction is based on a minimum model depth of 1 m. As the minimum depth increases, the minimum grid size also increases.

It was also found that the R&B boundary condition had to be applied to all the open boundaries of the regional model. Simulations were conducted by using the R&B forcing along the deep water open boundaries, with other nonforcing conditions along an open boundary perpendicular to shore. These simulations resulted in amplitudes and phases which, at some locations, were not consistent with observations and other model results. L&H concluded that the application of a nonforcing boundary condition could result in interior solutions to the tidal forcing that could be quite different from the actual tides.

In this paper, we continue our studies into the coupling of global and regional models using the R&B boundary condition. Specifically we modeled the western Florida shelf, which is known to resonate with the M_2 tide. Bottom friction is an important factor when dealing with a resonant shelf, and it was found that a frictional coefficient, which is inversely proportional to depth was required for the Florida shelf. We then performed the north-central GOM simulations again, as well as additional simulations for the Kenya Coast. The results from all these

simulations indicate that tidal forcing using the R&B boundary formulation worked well when a linear friction coefficient of 7.5×10^{-4} (m/s) was used.

THE REGIONAL MODEL

The numerical model used for the regional simulations is the two-dimensional, vertically integrated, finite-difference, hydrodynamic model described in L&H. The equations of motion are

$$\frac{\partial u}{\partial t} - fv + gD \frac{\partial H}{\partial x} = -Cu/D^n \quad (1)$$

$$\frac{\partial v}{\partial t} + fu + gD \frac{\partial H}{\partial y} = -Cv/D^n$$

where u and v are the x -directed and y -directed transports, f is the Coriolis parameter, g is gravitational acceleration, t is time, H is the sea surface elevation, D is the water depth, C is a bottom friction coefficient, n is an integer, and the RHS of the above expressions represent the horizontal bottom stresses in the x and y directions. In L&H, $n = 2$. The equation of continuity is

$$\frac{\partial u}{\partial x} + \frac{\partial v}{\partial y} + \frac{\partial H}{\partial t} = 0.$$

The formulation of the model is given in L&H. In this study, it was found that the resonating M_2 tide over the Florida shelf was quite sensitive to the parameterization of friction. Indeed, the M_2 tide over the Florida shelf could not be reproduced using L&H's friction formulation that was proportional to depth squared. Instead, we used a formulation that has friction inversely proportional to D (i.e., $n = 1$ in (1); Reid and Whitaker, 1981). Because of the sensitivity to friction, as well as the fact that the Florida shelf covered a large region in the north-south direction, the model was changed to spherical coordinates and enhanced to include a variable Coriolis parameter (see Reid and Whitaker, 1981). In this way, the nuances of different bottom friction formulations would not be confused with the results of spatially varying grid sizes and Coriolis effects.

As in our previous work, the R&B expression,

$$U = \pm(H-\eta)(gD)^{1/2} \quad (2)$$

is used to describe transports perpendicular to open water boundaries. Here U is the transport perpendicular to the boundary, η is the specified tidal height, and the expression is positive for open boundaries in the positive x and y directions but negative in the negative x and y directions. The above expression is a simple energy radiation condition that allows us to specify the transport U along the open boundary of the edge of a model grid cell by using the tidal height (from the global model of Schwiderski, 1981, 1983) and the sea surface elevation of the interior of the grid cell (determined from the model itself). Any waves that are reflected from the model bathymetry or coastline (the H component in the expression) are allowed to pass through the boundary while forcing is still provided by the tides (the η component of the expression).

TIDAL FORCING OF REGIONAL MODELS

Western Florida Shelf

The western Florida shelf (Fig. 1) was chosen as a region to be modeled because it is known that the shelf is highly resonant with the M_2 tide (Reid and Whitaker, 1981). In particular, it is the direct gravitational forcing (as opposed to forcing at the Yucatan and Florida Straits) that is responsible for the enhanced tidal heights over the shelf. Thus, it is of interest to test the ability of our coupling methodology to: (1) reproduce a resonant response and (2) produce the response only with forcing at the boundaries (i.e., by not including the direct body forcing).

The western Florida region consists of a wide, shallow shelf that is bordered on the north by the Florida panhandle and on the south by the deeper waters of the Florida Straits. The horizontal grid spacing for the model was one-eighth of a degree. The tidal amplitudes and phases were determined at each grid point at the end of 8 days of simulation time following L&H.

As mentioned previously, it was found that the M_2 tides could only be reproduced using the frictional formulation given in equation (1) with $n = 1$. A number of values for C were tested for both the M_2 and the O_1 tidal constituents. Figures 2 and 3 show the resulting tidal amplitudes and phases with $C = 7.5 \times 10^{-4}$ m/s. The model does a good job in reproducing the resonance of the M_2 tide (Fig. 2a). The propagation of the M_2 tide is seen to be from the south to the north. The O_1 amplitudes are small, with maximum amplitudes some 2 cm smaller than indicated by observations. The phases (Fig. 3b) show little variation throughout most of the study area.

Observed tidal constants were used to produce time histories of the M_2 and O_1 tides at Cedar Key and Naples, Florida. These are compared with the model-predicted variations in Figures 4 and 5. The model slightly overestimates the M_2 amplitudes while it underpredicts the

O₁ amplitudes. Although the percent error of the O₁ amplitude is significant, the absolute error is only ~3 cm. Also, the model M₂ tides precede the observed tides, with the greatest difference being at Naples (1 hr, or an 8% phase error). The O₁ phases at Cedar Key and Naples are within 10% of the observed phase.

The North-Central Gulf of Mexico

As a result of the modifications of the numerical model (friction formulation, variable Coriolis, and spherical coordinates), it was decided that the simulations of L&H in the north-central GOM should be performed again. The north-central gulf region encompasses a wide shelf off the Texas Coast, as well as a narrow shelf around the Mississippi Delta (Fig. 6). Maximum depths are greater than 2700 m while minimum depths are 2 m. The horizontal grid spacing for the model was one-eighth of a degree. The M₂ tidal amplitudes and phases (with $C = 7.5 \times 10^{-4}$ m/s) are shown in Figure 7. These are almost identical to our previous results. Figure 8 gives the model-predicted amplitudes and phases for the O₁ tidal constituent. The contour plot of the phases is rather complicated, but the variations throughout most of the study area are rather small, of the order of 8° (2%).

Observed tidal constants were used to produce time histories of the M₂ and O₁ tides at the coastal locations of Galveston, Texas, and Cat Island, Mississippi. A comparison of these actual tidal variations and those from our regional model are shown in Figures 9 and 10. The model slightly overestimates the M₂ amplitudes. Also, the model M₂ tide lags the observed tide at Galveston by 30 minutes (a 4% phase shift). The agreement for O₁ tide at Galveston is good, with a slight overestimate of the maximum tidal height. We also see that the model tide lags the observed O₁ tide. The model O₁ amplitude for Cat Island is somewhat too small, but the phase is almost exact. Overall, the model amplitudes and phases were within 10% of the observations.

Model Tuning

The simulations showed that the model-predicted M₂ tidal amplitudes tended to be slightly too large. On the other hand, the model-predicted O₁ amplitudes tended to be too small. However, the M₂ errors were less than 8% except at Cat Island (~20% error), and the absolute error at Cat Island was only ~1 cm. Similarly, the amplitude errors for the O₁ tide were less than 9% except at Naples (~25% error), and the absolute O₁ amplitude error at Naples was only ~3 cm.

It was found that the amplitude errors could be reduced by slightly modifying the drag coefficient C. Increasing the value of C provided better predictions for the M₂ tidal amplitude while decreasing the value of C provided better predictions of the O₁ tidal amplitude. This is a common phenomena, with current regimes oscillating at higher frequencies requiring larger drag

coefficients. For the modeling of more than one tidal species, an optimum value for C must be chosen to provide the best overall tidal predictions. If no data exist for tuning a regional model, then $C = 7.5 \times 10^{-4}$ m/s would be an appropriate value to use.

In order to determine if the model accuracy could be improved, other bottom friction parameterizations were considered. We began with the bottom friction of L&H that has the form of $(-C_u/D^2, -C_v/D^2)$. The inverse depth squared formulation is often used during the modeling of wind-driven situations to keep coastal grid points from going completely dry in the model. Test simulations showed that such a formulation was incapable of providing enough frictional damping over the resonant Florida shelf, regardless of the value of C . The model Florida shelf M_2 tidal amplitudes were close to twice observed values. We must conclude that frictional damping in the deeper waters of a resonating shelf are too important to use an inverse depth squared formulation for bottom friction.

We also performed a number of simulations using bottom friction in the form of $(-C(u^2+v^2)^{1/2}u/D, -C(u^2+v^2)^{1/2}v/D)$. This essentially allows friction to be a function of the magnitude of the current, which is commonly the case. However, coastal tidal currents tend to be relatively small, so the effects of the nonlinearity of friction may not be noticeable. This appears to be the case for our GOM regional models, for the simulations with this frictional formulation gave results that were virtually identical to those presented.

Tides on the Kenya Shelf

Based on the simulations of the Florida shelf and the north-central GOM, it was decided to attempt the modeling of the Kenya shelf using $C = 7.5 \times 10^{-4}$ m/s. The Kenya shelf drops off rather rapidly, reaching a depth of 1500 m only 110 km offshore. The Kenya model domain and bathymetry are shown in Figure 11. The grid spacing is one-eighth of a degree, both in latitude and longitude.

Simulations were run for the M_2 and K_1 tidal constituents. Observed M_2 tidal variations at the coastal stations of Shimoni and Kilifi (Fig. 11) are compared with the model predictions in Figure 12. The M_2 amplitude was slightly overpredicted at Shimoni and Kilifi (by 5% at both sites). There were small phase shifts at both stations. While the M_2 tides were slightly overpredicted, the K_1 tides (Fig. 13) were underpredicted (7% at Shimoni and 4% at Kilifi). The K_1 phase was shifted 3% at both stations. Overall, the coupling methodology appears to work quite well.

TIDAL FORCING OF SEMIENCLOSED BASINS

Our studies have also included the application of our coupling methodology to semienclosed basins. Basin modeling is of particular interest for a variety of reasons. Firstly, many basins must be forced at their entrances, which can be rather limited regions. L&H performed a test simulation of a closed channel that was forced at its open end. They showed that the R&B formulation introduces some modifications to the tidal forcing signal as a result of wave energy reflected from the end of the channel. In such cases, the tidal amplitudes all along the channel are considerably smaller than the results obtained analytically. Such a situation could result when forcing a regional model of a basin.

Secondly, some basins may be of such a size and have such spatially limited entrances that direct body forcing cannot be ignored when the R&B formulation is used at the entrances of the basin. To be sure, the tidal parameters at the basin entrances from a global model will contain some information related to tidal energy entering the basin and tidal energy resulting from direct forcing. However, the direct forcing energies at the mouth of a basin may not reflect significant amounts of the overall body forcing energies that are felt through the domain of the basin. In such a case, our methodology could not provide the required forcing to reproduce the observed tides within the basin.

We present two basin model tests. The first is for the Persian Gulf basin (Fig. 14). The Persian Gulf is a long, narrow, semienclosed basin that opens into the Arabian Sea via the Strait of Hormuz. The longitudinal axis of the Persian Gulf runs from the east to west-northwest. Maximum depths are slightly greater than 75 m, while most of the depths lie between 25 and 50 m. In many ways, the Persian Gulf is similar to the channel simulated by L&H. Unfortunately, the Persian Gulf was not included in the global model of Schwiderski (1983). Thus, the amplitudes and phases from the global tide model do not reflect the interaction between the Persian Gulf and the north Arabian Sea.

The second basin is the entire GOM. The semidiurnal tides within the GOM are primarily driven by direct body forcing. Thus, the GOM provides a good test to ascertain the ability of the R&B boundary formulation to drive the entire basin by forcing only at the Yucatan and Florida Straits.

A Persian Gulf Regional Model

A regional model was set up for the Persian Gulf using the numerical model described previously. The grid spacing was one-tenth of a degree, both in latitude and longitude. The stations that were used to compare observed versus model-predicted values are Saffaniya,

Bushehr, and Lavar (Fig. 14). Simulations were run for two different boundary configurations, for the M₂ tide. The first configuration consisted of open-water boundaries in the Arabian Sea, 82 km from the mouth of the Strait of Hormuz and extending 255 km to the south. The second configuration was a north-south boundary across the narrowest portion of the Strait of Hormuz, approximately 70 km in length.

Driving the model with the first configuration of two boundaries in the Arabian Sea yields the amplitude contours shown in Figure 15. The maximum amplitude occurs in the Strait of Hormuz, greater than 70 cm. Two amphidromic points are indicated, one in the north and another in the south. Data shown in the Admiralty Tide Tables (1982) indicate that the pattern is correct, but the amplitudes are too small. Observed and modeled tidal variations are shown in Figure 16. These also point out the degree of underestimating the tidal amplitude as well as errors in the tidal phase.

The tidal forcing at the open boundaries of the above simulations were increased until the implicit solutions of the tidal amplitude at the open boundaries match those given by the Schwiderski model. This resulted in some improvement in the predicted amplitudes, but the errors were still relatively large. This may be just the result of the fact that the global model did not include the Persian Gulf. The model was then forced at the Straits of Hormuz to determine if realistic fluctuations could be obtained. In order to drive the model from the Strait of Hormuz, tidal constants obtained from the Admiralty Tide Tables were used. Thus, the simulation does not represent coupling between the regional and global models. The model produced an average amplitude value across the Strait of Hormuz that was 50% lower than the input values from the Admiralty Tide Tables, and the amplitudes throughout the domain of the model were significantly lower than the Arabian Sea simulations. However, the phases are much more accurate, with a 2% maximum phase shift. When the amplitudes at the Straits of Hormuz were increased, the model still underestimated the amplitudes at all the stations.

The Gulf of Mexico Regional Model

The GOM is a large semiclosed basin with two relatively small openings (Fig. 17). The Florida Straits are a little over 200 km wide and are ~2000 m deep. The Yucatan Straits are a little less than 200 km wide and are ~2000 m deep. The basin has some broad shelves and some narrower shelves and has a maximum depth about 3600 m.

A number of stations were used to compare observed versus model-predicted tidal amplitudes and phases, and these are also shown in Figure 17. Three simulations were run for the M₂ tidal constituent. The first consisted of forcing from the open water boundaries across the Yucatan and Florida Straits (port forcing) using the R&B formulation and the tidal parameters

from the Schwiderski global model. The second simulation consisted of direct gravitational forcing, without port forcing. The third scenario consisted of both direct and port forcing.

The model used in these simulations is the one discussed by Blumberg and Mellor (1987). The model used in all the previous simulations uses an implicit, alternating direction solution scheme that has been shown to generate spurious basin modes in the GOM as a result of the solution technique (Reid and Whitaker, 1981). Thus, we use the Blumberg-Mellor model, which is a fully nonlinear, hydrodynamic model, that uses an explicit solution scheme. The model was run in its two dimensional mode with bottom friction parameterized as $(-C(u^2+v^2)^{1/2}u/D, -C(u^2+v^2)^{1/2}v/D)$. The value of C was 2.5×10^{-3} .

The model was forced at the Florida and Yucatan Straits, and the results are shown in Figure 18. It can be seen that the amplitudes over the Florida shelf are significantly underestimated while the phase is reasonably correct at all the stations. These results have been tuned so that the resultant amplitudes at both the Florida and Yucatan Straits match the Schwiderski values. The tuning is obtained by multiplying the Schwiderski amplitudes at the ports by approximately 2.

Direct gravitational forcing was added to the model (Reid and Whitaker, 1981), and a radiation boundary condition was used at the two ports. Before conducting any simulations, the direct gravitational forcing parameters (amplitude and phase) must be adjusted to account for the influence of friction. The results of Reid and Whitaker (1981) indicate that the amplitudes should be reduced by a factor of 0.6 and the phases should be shifted by $\sim 20^\circ$. A simulation was made with the body forcing adjusted as suggested in Reid and Whitaker, and there was no port forcing. The results (Fig. 19) show that the amplitudes are significantly underestimated at the ports and at Campeche, while the phase is off considerably at most of the stations. Again, it is important to point out that these results have already been tuned based on the results of Reid and Whitaker (1981).

Combining the tuned port and direct forcing yields the results shown in Figure 20. The agreement between the model results and observations is reasonable, but it is obvious that additional tuning is required.

DISCUSSION

Several other test simulations were made to test the R&B condition using the Florida and central GOM regional models. The models were run using the M_2 forcing and Eq. (2) as the boundary condition but with $H = 0$ corresponding to the traditional height specified boundary condition. This allowed the tidal energy to enter the model domains but did not allow any wave energy approaching the open boundaries to leave the model domains. As expected, the results

were quite different than those shown in Figures 2 and 7, the amplitudes being far too large. For the north-central GOM model, the tidal amplitudes ranged from 50 to >250 cm.

Other simulations were patterned after those of L&H in which either a simple radiation condition or a zero-gradient condition was applied to the eastern boundary of the north-central GOM model. In L&H, the M₂ tide was simulated using these nonforcing boundary conditions, and the results were solutions that were different than the actual tides or other model results. These tests were repeated with the radiation and zero-gradient conditions along the western open boundary of the model. This was done since the M₂ tide propagates from east to west in the model domain, and it is conceivable that better predictions could be obtained with such boundary conditions. The results, however, do not bear this out. The amplitudes and phases in the western part of the model had some notable differences from the results given by Reid and Whitaker (1981) and those shown in Figure 7.

Overall, the numerical simulations indicate that the Reid and Bodine open boundary condition can be quite effective in coupling a regional model with a global tidal model. This appears to be true for the semidiurnal and diurnal tides in our GOM and Kenya Coast test regions.

As for the basin studies, neither the Persian Gulf nor the GOM provided good results when driven only by the Schwiderski tidal constants using the R&B condition. While the phase shifts for the Persian Gulf were acceptable, several of the stations had significant amplitude discrepancies ranging from 24-45%, with absolute errors over 10 cm. And even though a reasonably accurate GOM model could be developed by the incorporation of direct body forcing, it is seen that a tuning process is still required.

The Persian Gulf, which is geometrically similar to the channel problem discussed by L&H, exhibits tidal behavior similar to the channel problem (e.g., amplitudes at the mouth that are ~60% of the appropriate value). If this is true, we cannot expect accurate amplitudes and phases without adjustment of the global model parameters used to drive the model at the mouth of the gulf. On the other hand, we also cannot discount the possibility that the problem lies with the fact that Schwiderski's global model did not include the Persian Gulf.

CONCLUSIONS

Our results indicate that the Reid and Bodine open boundary formulation is quite effective in driving a regional model using parameters from a global model. Test simulations with a zero-gradient or radiation boundary condition at some of the model open boundaries confirm the findings of L&H: the R&B formulation should be applied at all the open boundaries to obtain the most accurate estimates of tidal amplitudes and phases. The application of the R&B formulation

to semienclosed basins required considerable tuning and, therefore, should be used with great care.

REFERENCES

Admiralty Tide Tables (1982). Atlantic and Indian Oceans, Vol. 2. Published by the Hydrographer of the Navy, Royal Navy, 202-282.

Blumberg, A. F. and G. L. Mellor (1987). A description of a three-dimensional coastal ocean circulation model. In *Three-Dimensional Coastal Ocean Models* (N. S. Heaps, ed.). Amer. Geophys. Un., Washington, DC, 1-16.

Lewis, J. K. and Y. L. Hsu (1990). Developing a coupled regional tide model. Candidate report, Naval Oceanographic and Atmospheric Research Laboratory (submitted 1/91), 15 pp.

Reid, R. O. and B. R. Bodine (1968). Numerical model for storm surges in Galveston Bay. ASCE, *J. Water. and Harb. Div.*, 94, 33-57.

Reid, R. O. and R. E. Whitaker (1981). Numerical model for astronomical tides in the Gulf of Mexico. Report by Dept. of Ocean., Texas A&M Univ., to the U.S. Army Engineer, Waterways Exp. Station, Vicksburg, MS, 115 pp.

Schwiderski, E. W. (1981). Global ocean tides, Part V: the diurnal principal lunar tide O_1 , atlas of tidal charts and maps. Naval Surface Weapons Center, Silver Spring, MD. NSWC Tech. Rep. 81-144, 15 pp.

Schwiderski, E. W. (1983). Atlas of ocean tidal charts and maps, Part I: the semi-diurnal principal lunar tide M_2 . *Mar. Geodesy*, Vol. 6, 219-265.

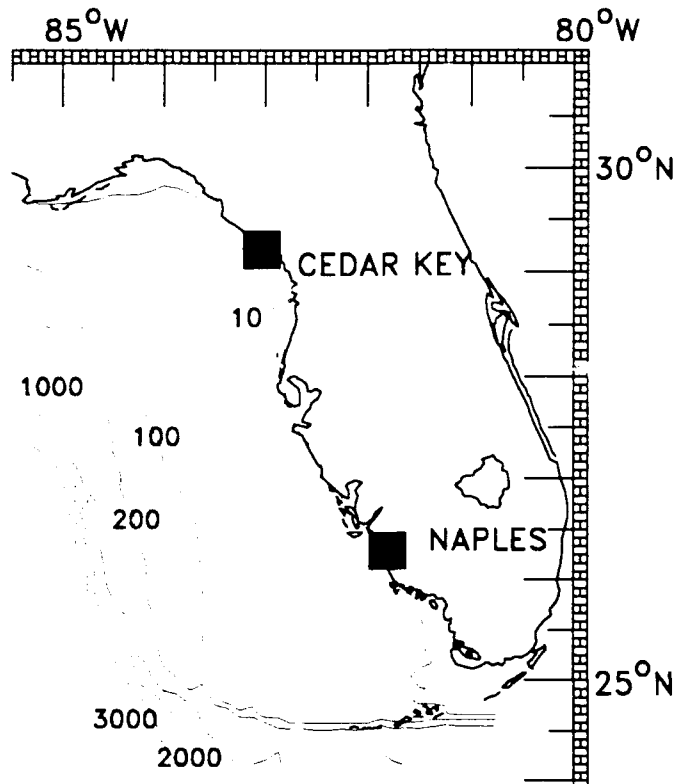


Fig. 1. Bathymetry (m) for the Florida shelf regional model.

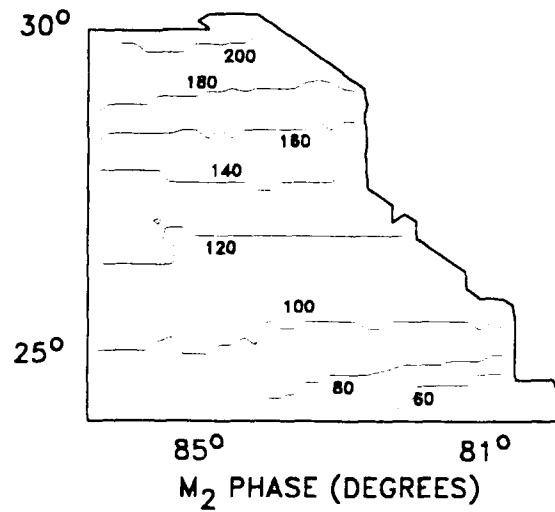
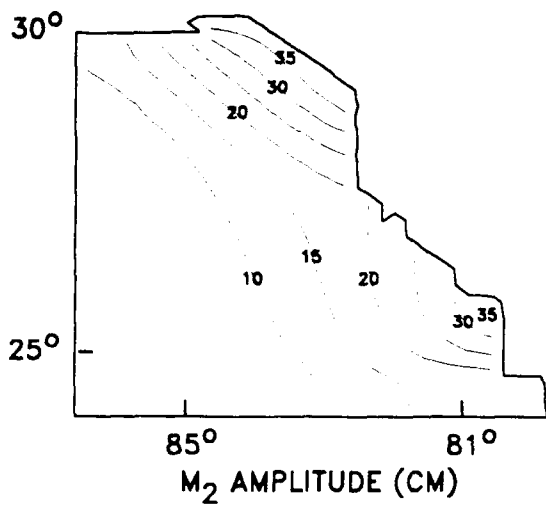


Fig. 2. M₂ tide on the west Florida shelf according to the regional model using the Reid and Bodine boundary condition with the Schwiderski tidal constants.

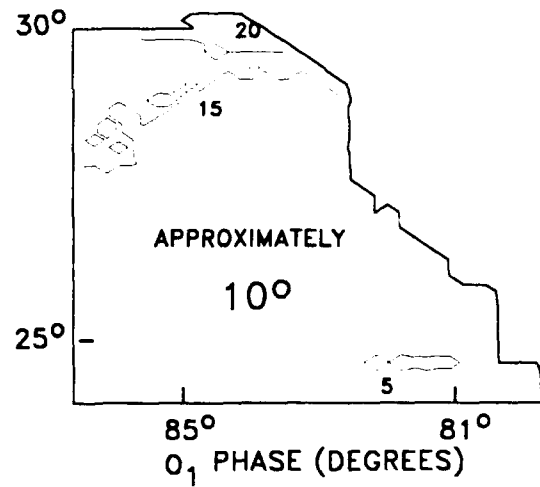
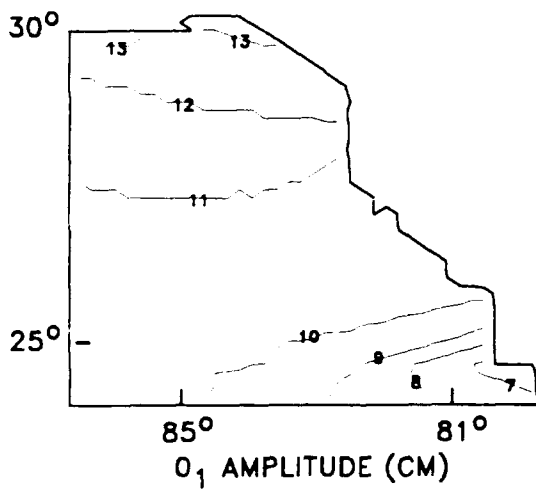


Fig. 3. O₁ tide on the west Florida shelf according to the regional model using the Reid and Bodine boundary condition with the Schwiderski tidal constants.

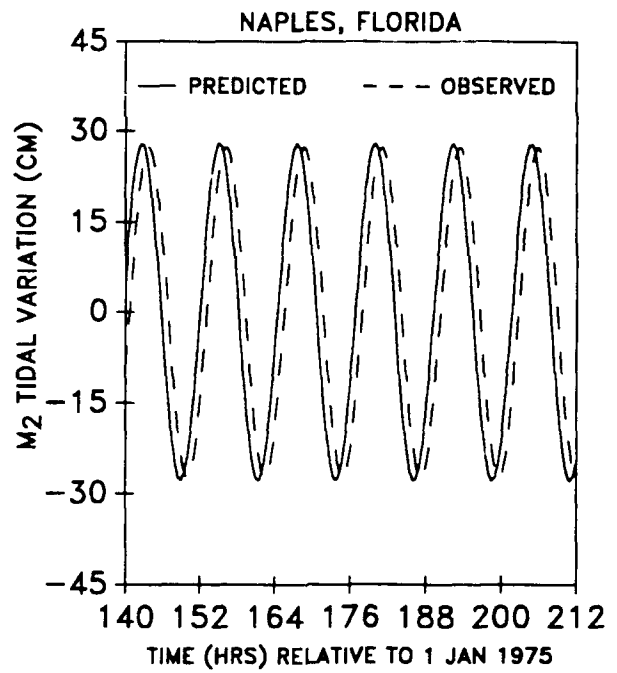
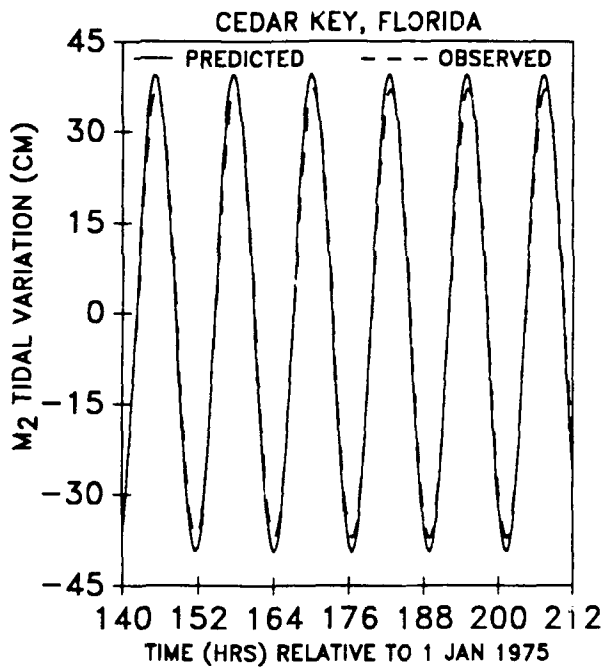


Fig. 4. A comparison of the M_2 tide levels from the Florida shelf regional model and those predicted by the observed tide amplitudes and phases at Cedar Key and Naples, Florida.

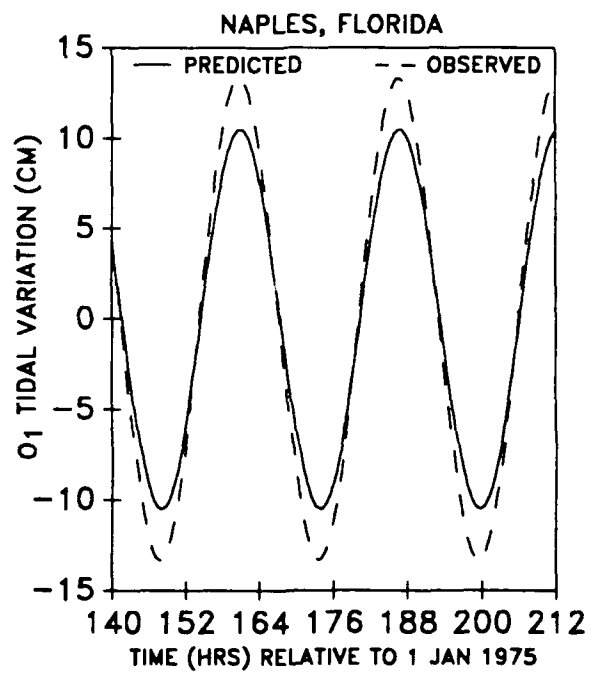
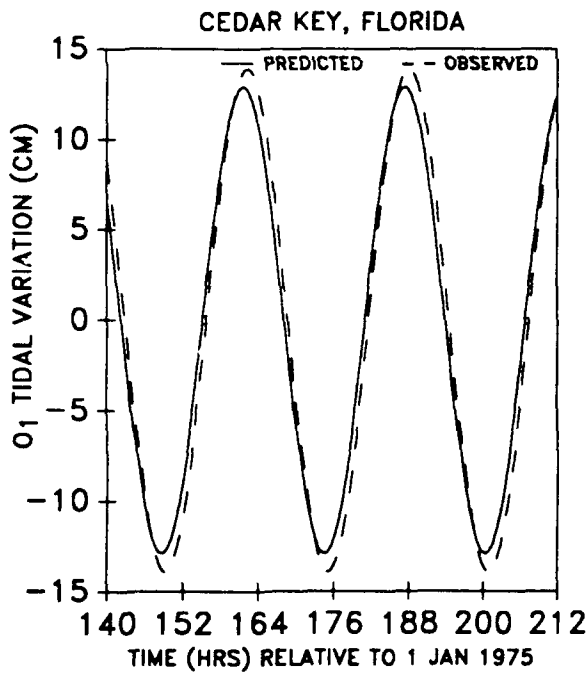


Fig. 5. A comparison of the O_1 tide levels from the Florida shelf regional model and those predicted by the observed tide amplitudes and phases at Cedar Key and Naples, Florida.

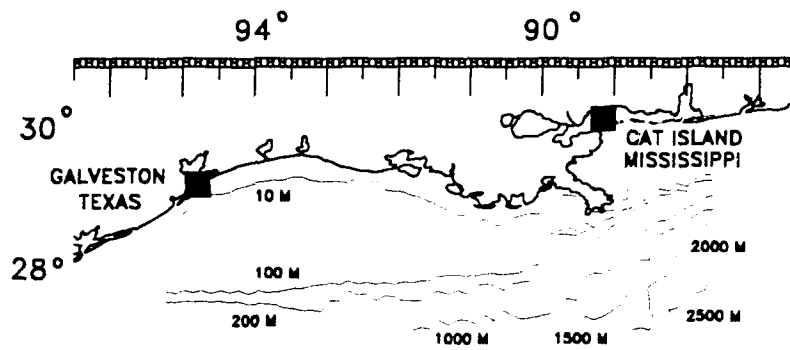


Fig. 6. Bathymetry for the north-central GOM regional model.

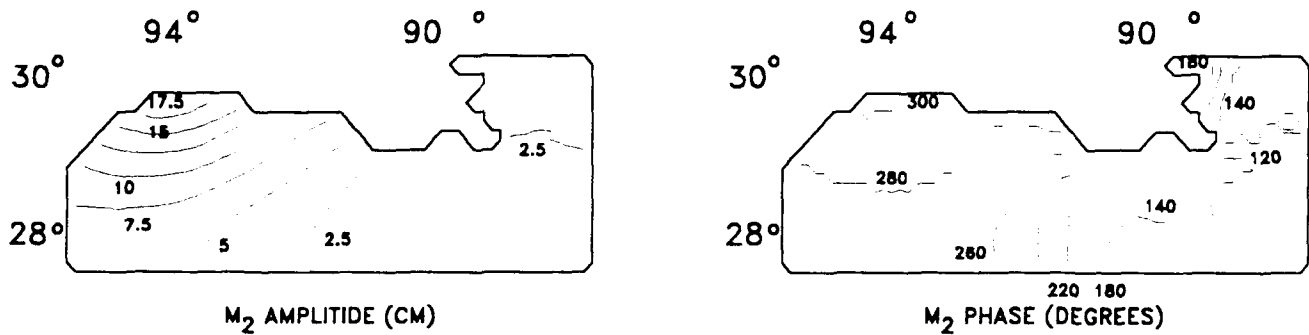


Fig. 7. M_2 tide for the north-central GOM according to the regional model using the Reid and Bodine boundary condition with the Schwiderski tidal constants.

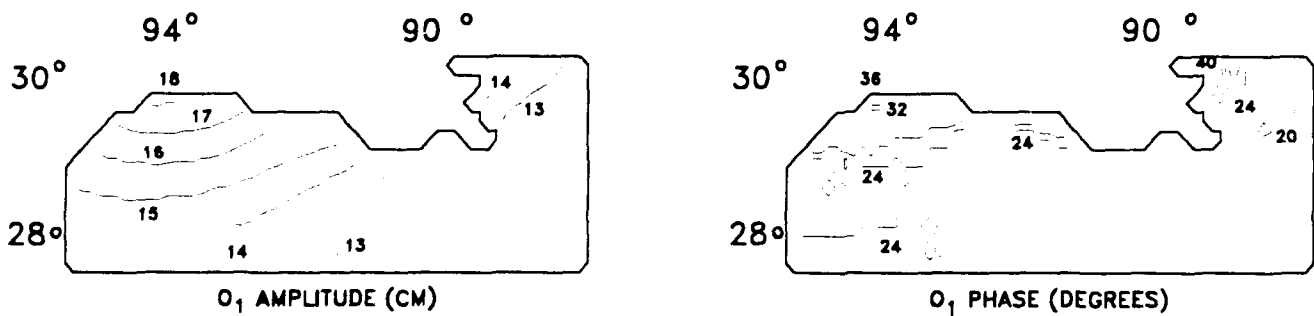


Fig. 8. O_1 tide in the north-central GOM according to the regional model using the Reid and Bodine boundary condition with the Schwiderski tidal constants.

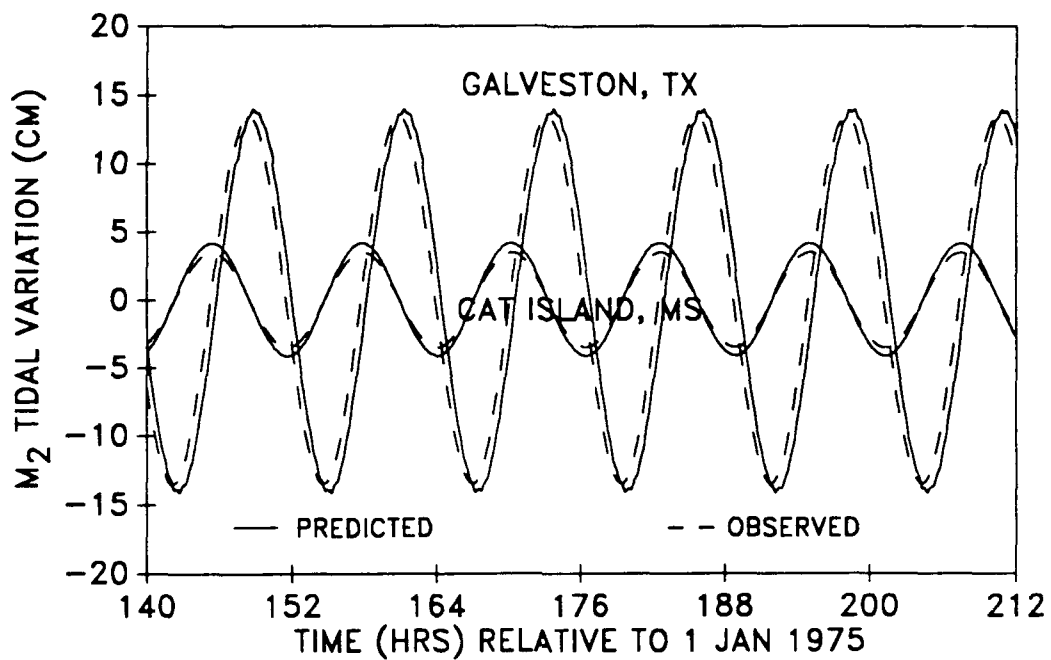


Fig. 9. A comparison of the M_2 tide levels from the north-central GOM regional model and those predicted by the observed tide amplitudes and phases at Galveston, Texas and Cat Island, Mississippi.

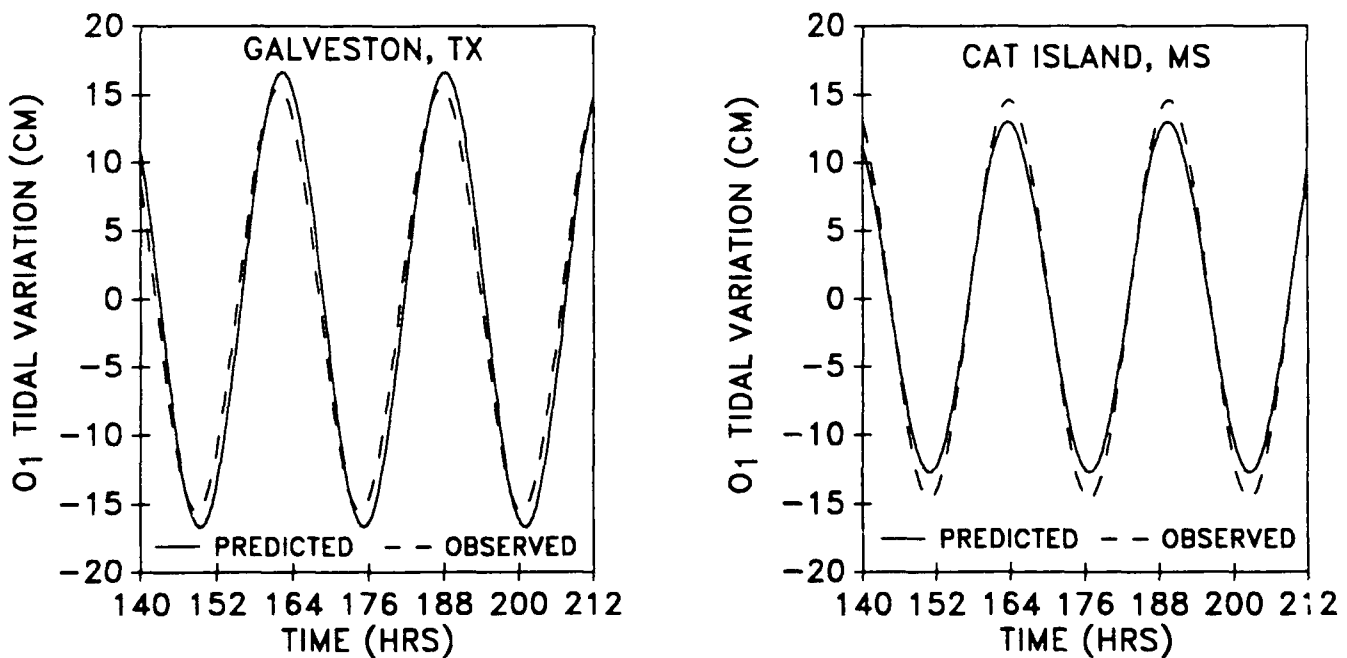


Fig. 10. A comparison of the O_1 tide levels from the north-central GOM regional model and those predicted by the observed tide amplitudes and phases at Galveston, Texas and Cat Island, Mississippi.

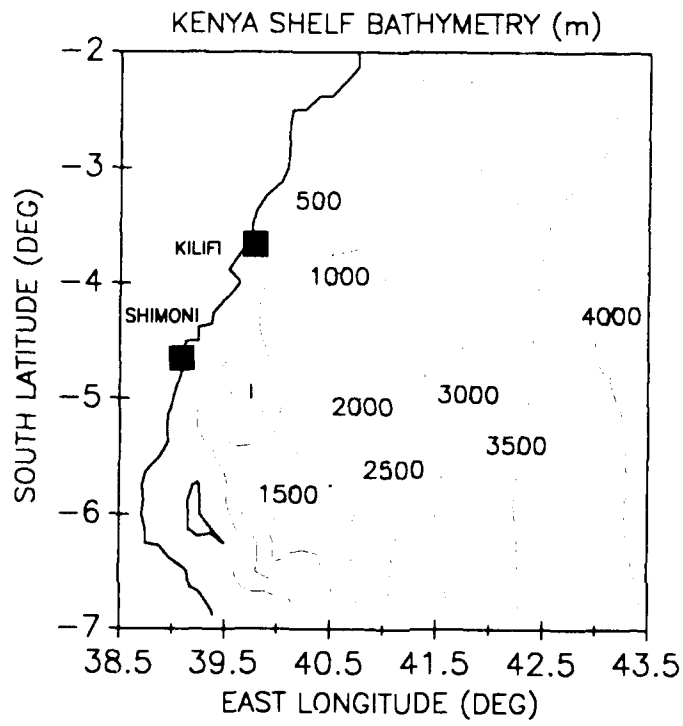


Fig. 11. Bathymetry for the Kenya Coast regional model.

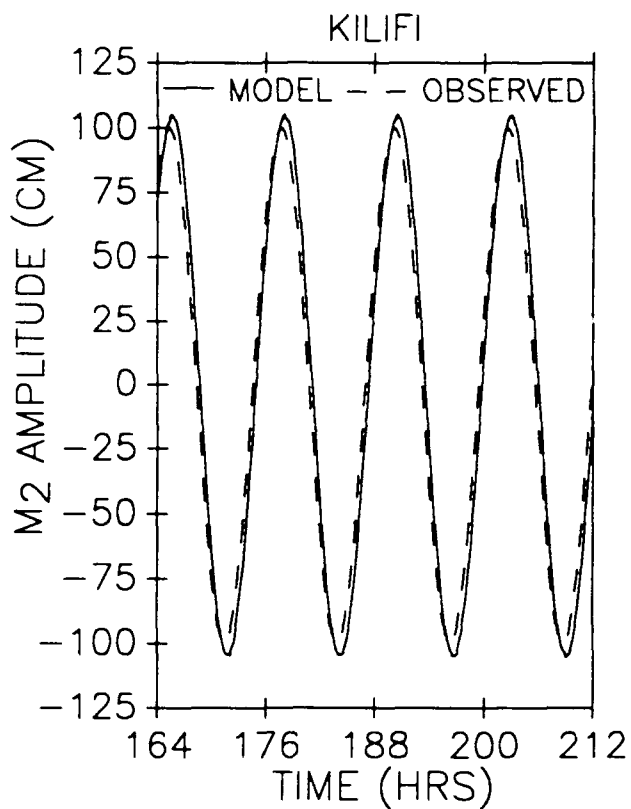
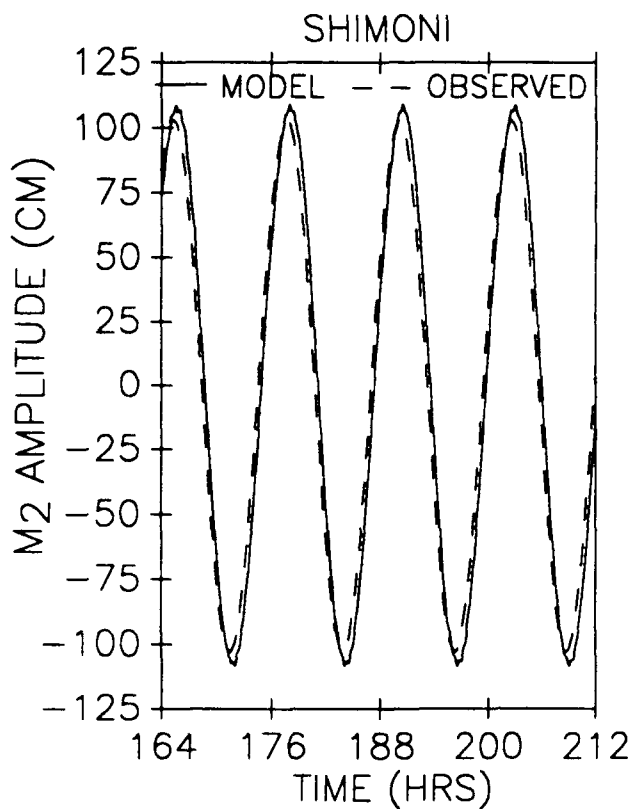


Fig. 12. A comparison of the M₂ tide levels from the Kenya Coast regional model and those predicted by the observed tide amplitudes and phases at Shimoni and at Kilifi.

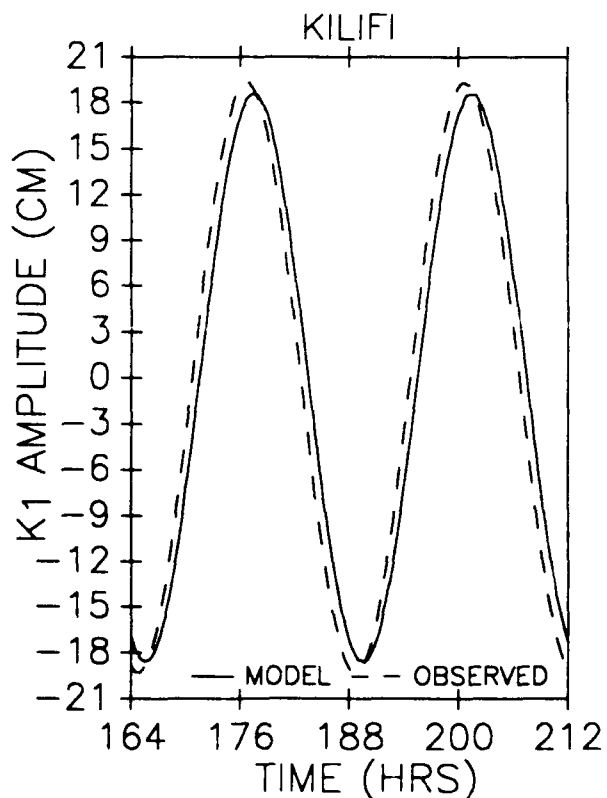
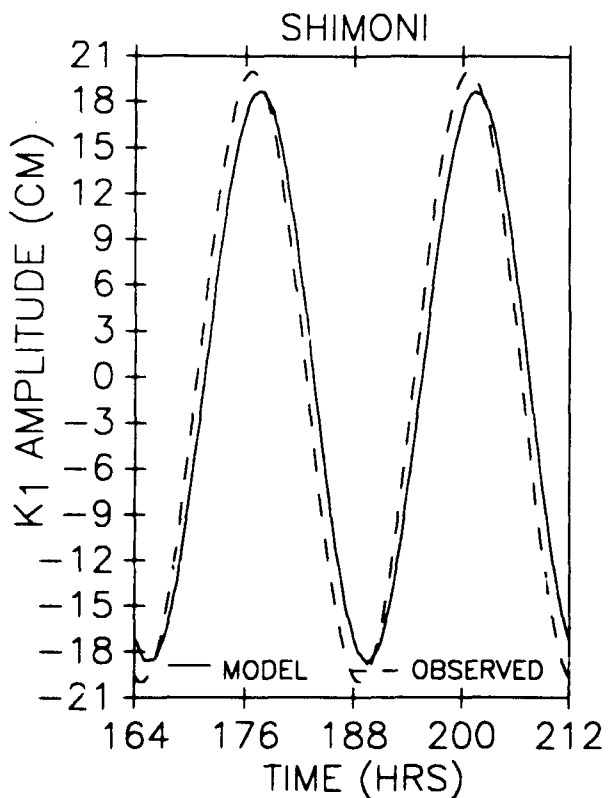


Fig. 13. A comparison of the K₁ tide levels from the Kenya Coast regional model and those predicted by the observed tide amplitudes and phases at Shimoni and at Kilifi.

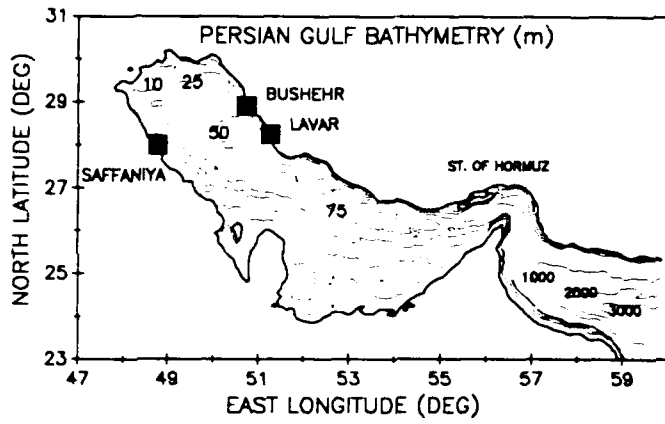


Fig. 14. Bathymetry for the Persian Gulf regional model.

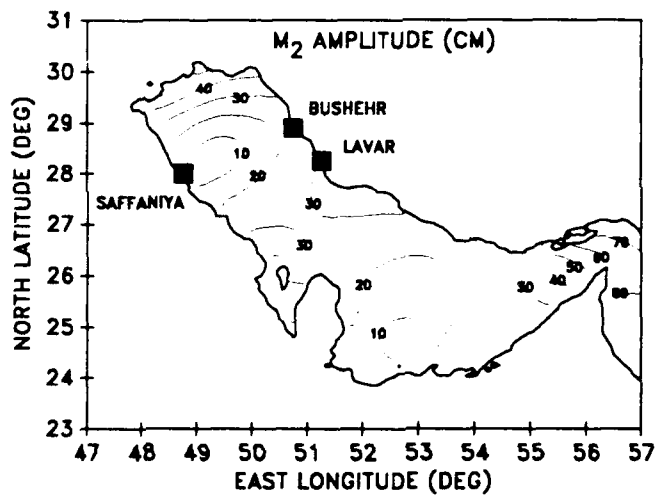


Fig. 15. M₂ amplitude contours for the Persian Gulf when the regional model is driven from the Arabian Sea.

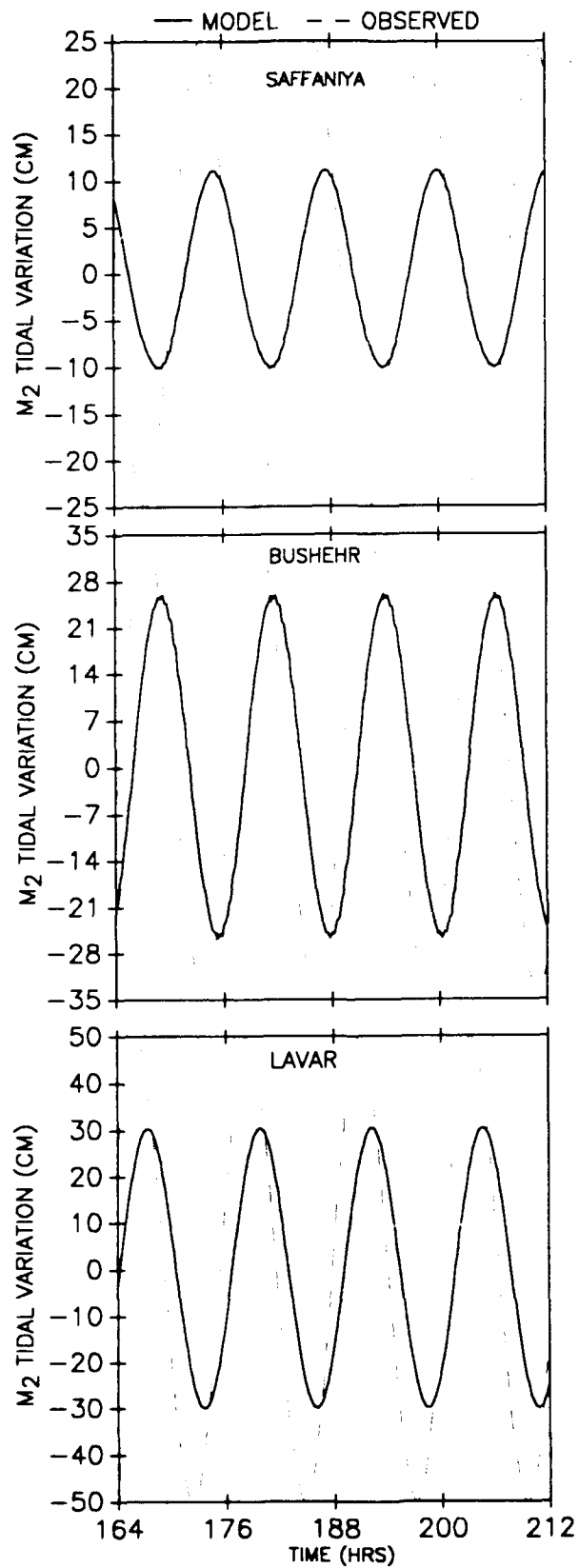


Fig. 16. A comparison between the observed and model-predicted M₂ tide variations from the Persian Gulf regional model at Saffaniya, Bushehr, and Lavar when the model is driven from the Arabian Sea.

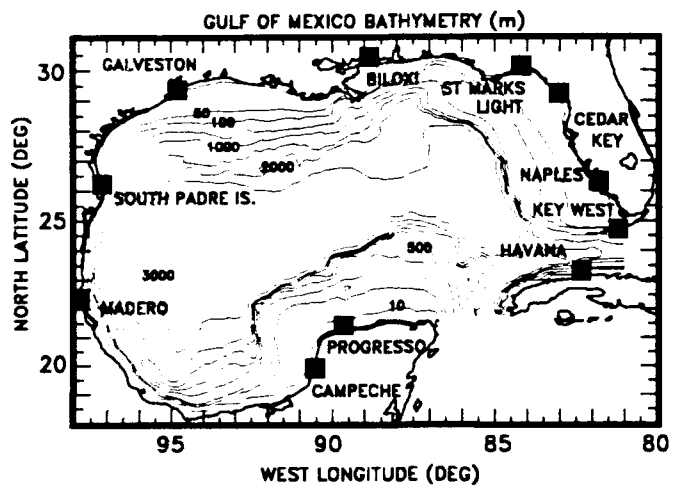


Fig. 17. Bathymetry for the Gulf of Mexico basin model.

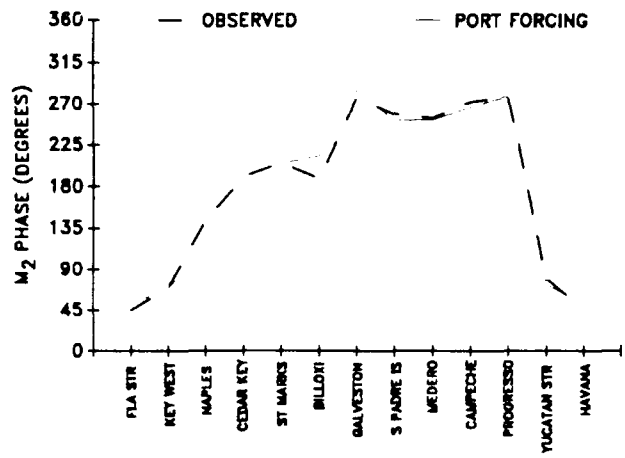
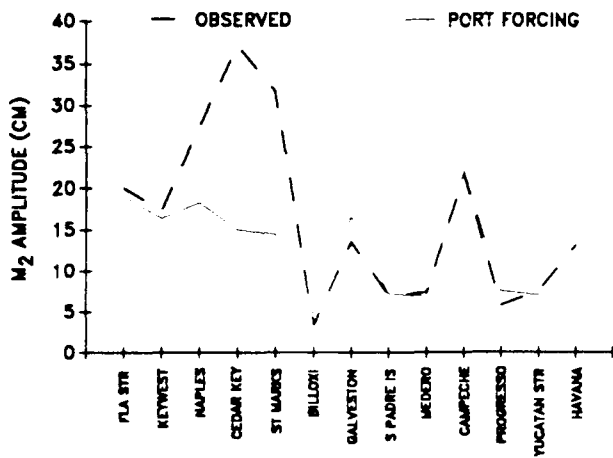


Fig. 18. A comparison between the observed and model-predicted M_2 tide variations from the Gulf of Mexico basin model for various stations along the Gulf of Mexico when the model is driven at the Yucatan and Florida Straits.

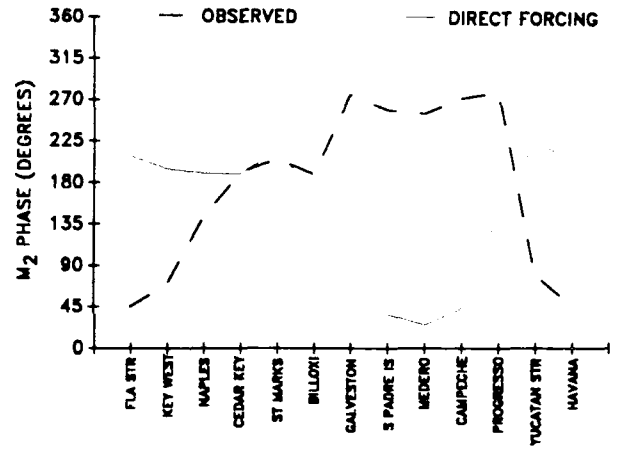
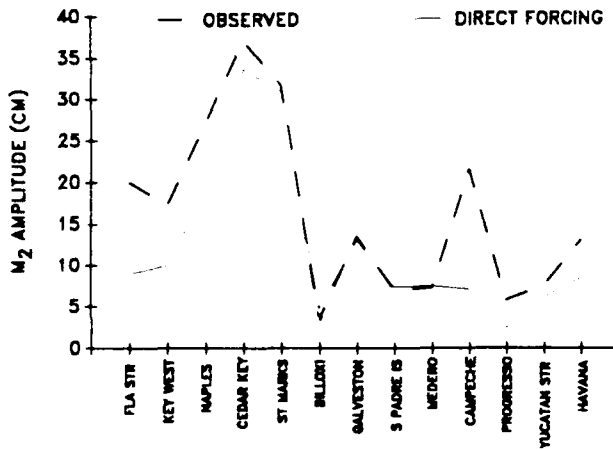


Fig. 19. A comparison between the observed and model-predicted M_2 tide variations from the Gulf of Mexico basin model for various stations along the Gulf of Mexico when the model is driven by direct gravitational forcing.

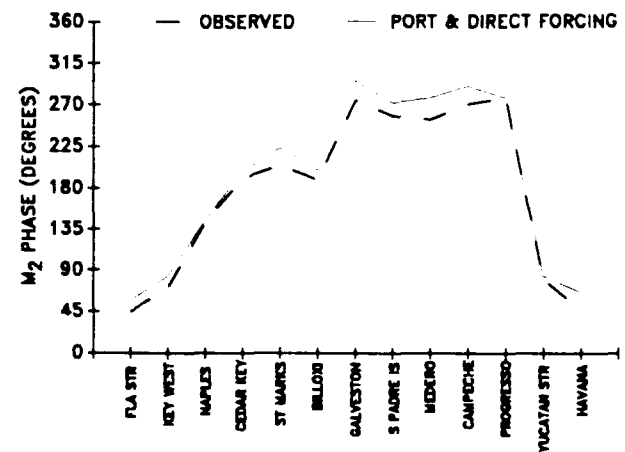
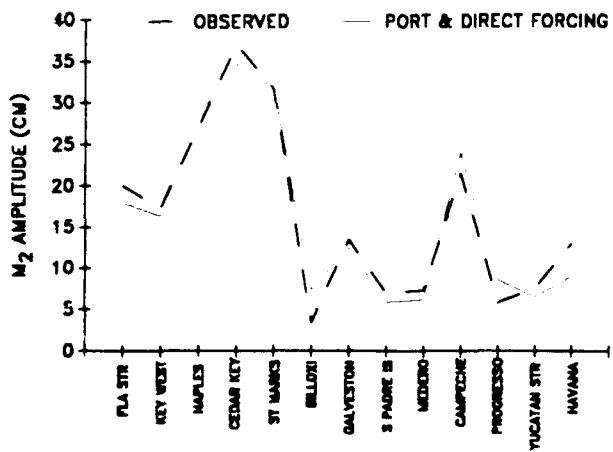


Fig. 20. A comparison between the observed and model-predicted M_2 tide variations from the Gulf of Mexico basin model for various stations along the Gulf of Mexico when the model is driven by both the port and direct gravitational forcing.

DISTRIBUTION LIST

Naval Oceanographic Office
Stennis Space Center, MS 39522-5001

Attn: Code H
Code HD
Code HDD
Code OP
Code OWPS
Code TD
Library (2)

Naval Research Laboratory
Stennis Space Center, MS 39529-5004

Attn: Code 113
Code 300
Code 350
Code 352
Code 125L(10)
Code 125P
Code 401

Office of Naval Technology
800 N. Quincy St.
Arlington, VA 22217
Attn: Code 234, Dr. T. Warfield

Naval Research Laboratory
Washington, DC 20375
Attn: Library

REPORT DOCUMENTATION PAGE

Form Approved
OBM No. 0704-0188

Public reporting burden for this collection of information is estimated to average 1 hour per response, including the time for reviewing instructions, searching existing data sources, gathering and maintaining the data needed, and completing and reviewing the collection of information. Send comments regarding this burden or any other aspect of this collection of information, including suggestions for reducing this burden, to Washington Headquarters Services, Directorate for Information Operations and Reports, 1215 Jefferson Davis Highway, Suite 1204, Arlington, VA 22202-4302, and to the Office of Management and Budget, Paperwork Reduction Project (0704-0188), Washington, DC 20503.

1. Agency Use Only (Leave blank).		2. Report Date. January 1992		3. Report Type and Dates Covered. Final	
4. Title and Subtitle. A Coupled Regional Tide Model				5. Funding Numbers. Program Element No. 0602435N Project No. RM35G81 Task No. M0G Accession No. DN251010 Work Unit No. 13522D	
6. Author(s). J.K. Lewis*, G.A. Vayda*, and Y.L. Hsu**				8. Performing Organization Report Number. NOARL Technical Note 221	
7. Performing Organization Name(s) and Address(es). SAIC 833 Hancock Square, Suite B Bay St. Louis, Mississippi 39520 Naval Oceanographic and Atmospheric Research Laboratory Ocean Science Directorate Stennis Space Center, Mississippi 39529-5004				10. Sponsoring/Monitoring Agency Report Number. NOARL Technical Note 221	
9. Sponsoring/Monitoring Agency Name(s) and Address(es). Naval Oceanographic and Atmospheric Research Laboratory Exploratory Development Program Group Stennis Space Center, MS 39529-5004				11. Supplementary Notes. *SAIC 833 Hancock Square, Suite B Bay St. Louis, Mississippi 39520 **Naval Oceanographic and Atmospheric Research Laboratory Ocean Science Directorate Stennis Space Center, Mississippi 39529-5004	
12a. Distribution/Availability Statement. Approved for public release; distribution is unlimited.				12b. Distribution Code.	
13. Abstract (Maximum 200 words). Two-dimensional numerical models were used to further study appropriate conditions at the open boundaries for regional models forced by parameters from a global tidal model. The open boundary condition of Reid and Bodine (1968) was applied to regional models of the western Florida shelf, north-central Gulf of Mexico, and the Kenya Coast. In addition, two semienclosed basins were modeled, the Persian Gulf, and the entire Gulf of Mexico. A number of tests were conducted to determine how well forcing, using the tidal constants from the 1°x1° Schwiderski global model (1981, 1983) could reproduce regional tides as determined from observations. As seen in our previous work, the Reid and Bodine formulation was quite effective in driving the regional models while still allowing wave energy to propagate through the open boundaries and out of the model. The western Florida shelf is known to resonate with the M ₂ tide. Under such circumstances, the bottom friction becomes quite important in obtaining correct predictions of the observed tidal amplitudes. Several bottom friction schemes with varying drag coefficients were tested for both the north-central gulf and Florida shelf models. The results are discussed in light of the fact that we seek one scheme that would be applicable for both resonant and nonresonant situations. In the basin modeling experiments, the M ₂ tide could not be reproduced by forcing with just the Schwiderski tidal constants at the open boundaries. Perhaps the most significant problem with the Persian Gulf is the fact that it is not included in Schwiderski's global model. As for the entire Gulf of Mexico, direct gravitational forcing of the water is found to be critically important. Apparently the effect of this direct gravitational forcing does not result in a large enough signal at the Yucatan and Florida Straits such that this basin-wide model can be reproduced by forcing only at these two open boundaries.					
14. Subject Terms. Global Modeling, Air-Sea Interaction, Fine Mesh Modeling, Tide Modeling				15. Number of Pages. 23	
				16. Price Code.	
17. Security Classification of Report. Unclassified		18. Security Classification of This Page. Unclassified		19. Security Classification of Abstract. Unclassified	
				20. Limitation of Abstract. SAR	